ESI material for

Enantioseparation and chiral induction in Ag_{29} nanoclusters with intrinsic chirality

Hiroto Yoshida,[a] Masahiro Ehara,[b] U. Deva Priyakumar,[c] Tsuyoshi Kawai*[a] and Takuya Nakashima*[a]*

[a]Division of Materials Science, Graduate School of Science and Technology, Nara Institute of Science and Technology (NAIST), Ikoma, Nara 630-01921, Japan.

[b]Institute for Molecular Science, Research Center for Computational Science, Myodai-ji, Okazaki 444-8585, Japan.

[c]Centre for Computational Natural Sciences and Bioinformatics, International Institute of Information Technology, Hyderabad 500032, India

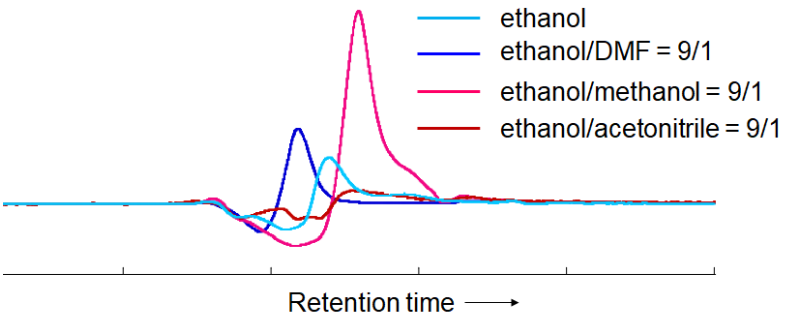

Fig. S1 Comparison of chiral HPLC chromatograms of $Ag_{29}(BDT)_{12}(TPP)_4$ NCs monitored by CD detector (at 450 nm) using ethanol, ethanol/DMF (9/1), ethanol/methanol (9/1) and ethanol/acetonitrile (9/1). The addition of second solvent (10 vol%) did not much improve the peak separation compared to ethanol.

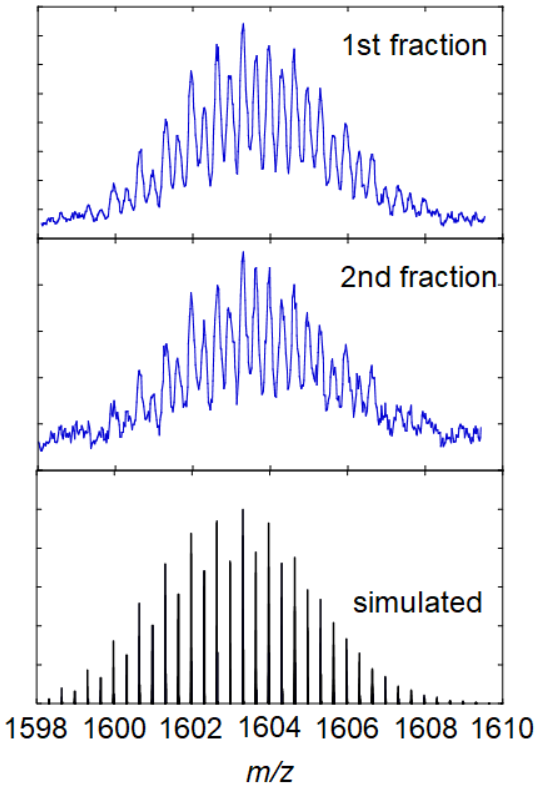

Fig. S2 ESI-MS of the first and second fractions together with the simulated isotope peak pattern with $[Ag_{29}(BDT)_{12}]^{3-}$.

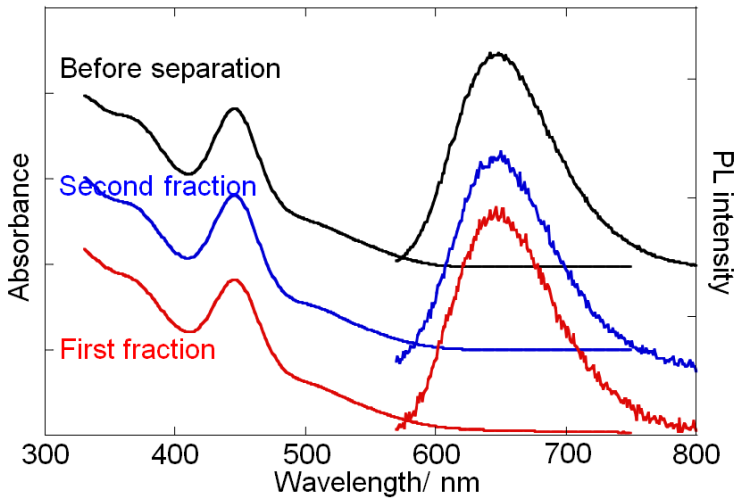

Fig. S3 (a) UV-vis and (b) photoluminescence spectra of $Ag(BDT)_{12}(TPP)_4$ NCs before enantioseparation in DMF together with NC-samples after separation in 10 mM TPP solution in DMF.

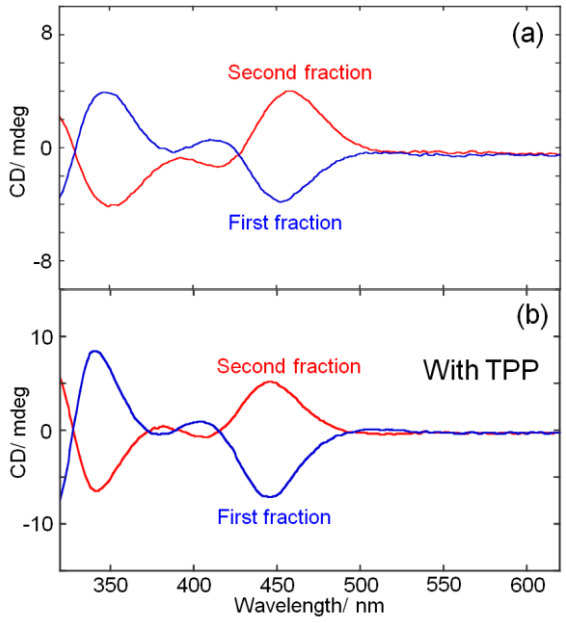

Fig. S4 CD spectra of NCs separated by the chiral HPLC after re-dispersion in (a) DMF and (b) DMF-TPP (10 mM) solutions.

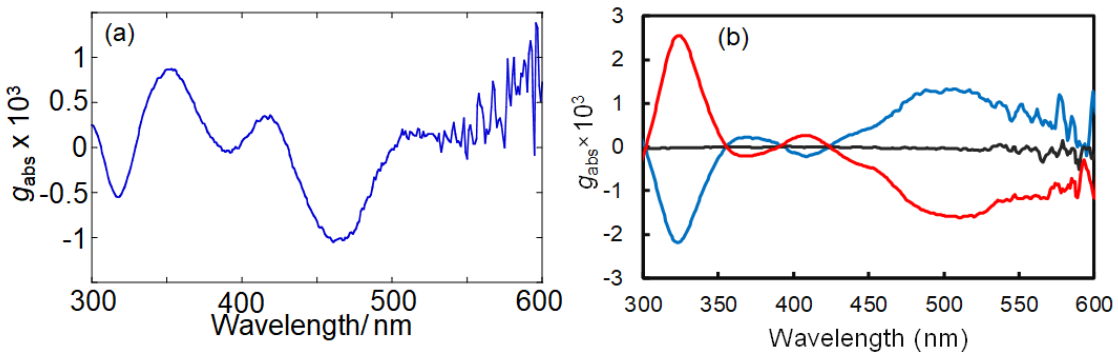

Fig. S5 (a) Apparent g_{abs}-spectrum of the first fraction and (b) g_{abs}-spectra of $Ag_{29}(DHLA)_{12}$ NCs in water. blue: Ag_{29}(*R*-DHLA)$_{12}$ NCs, red: Ag_{29}(*S*-DHLA)$_{12}$ NCs, black: Ag_{29}(*rac*-DHLA)$_{12}$ NCs.

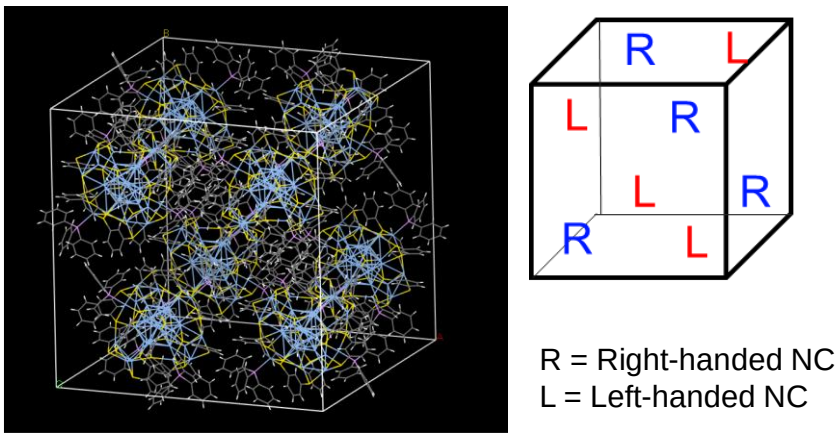

Fig. S6 Packing structure in the single crystal of $Ag_{29}(BDT)_{12}(TPP)_4$ NCs.
(Crystal data was referred to M. Bakr et al., *J. Am. Chem. Soc.* **2015**, 137, 11970-11975.)

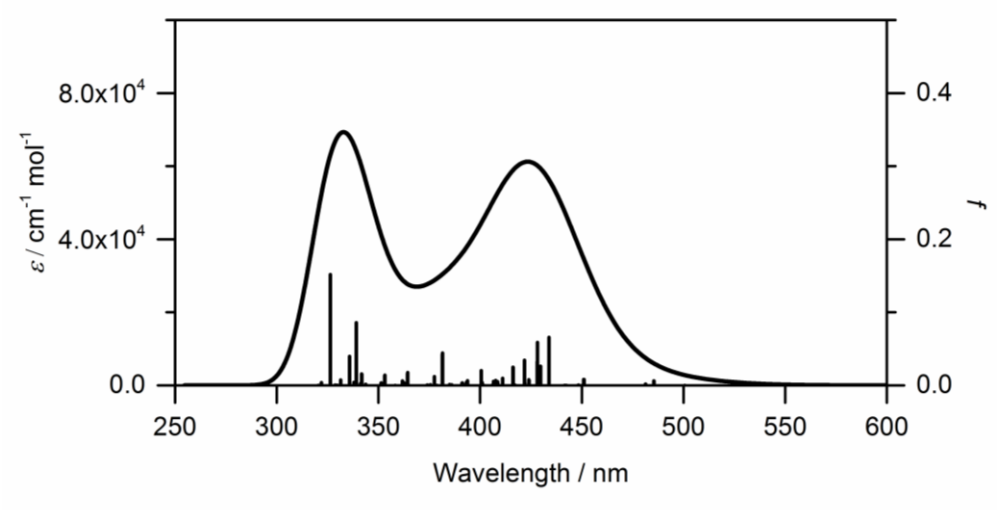

Fig. S7 Simulated UV-vis spectrum for the R-NC model.

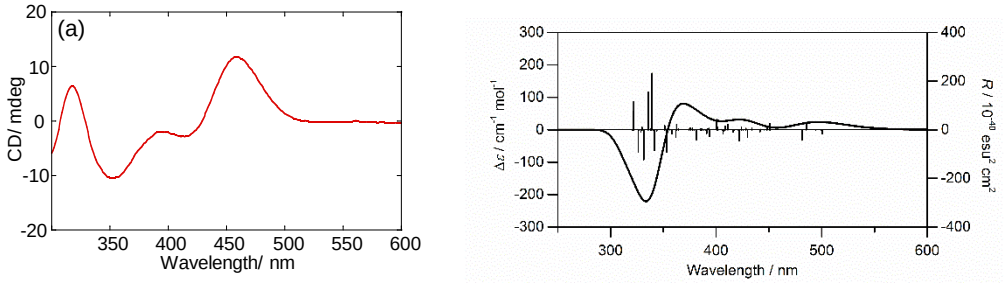

Fig. S8 (a) CD spectrum of the second fraction in ethanol. (b) Simulated CD spectrum based on the L-NC model structure.

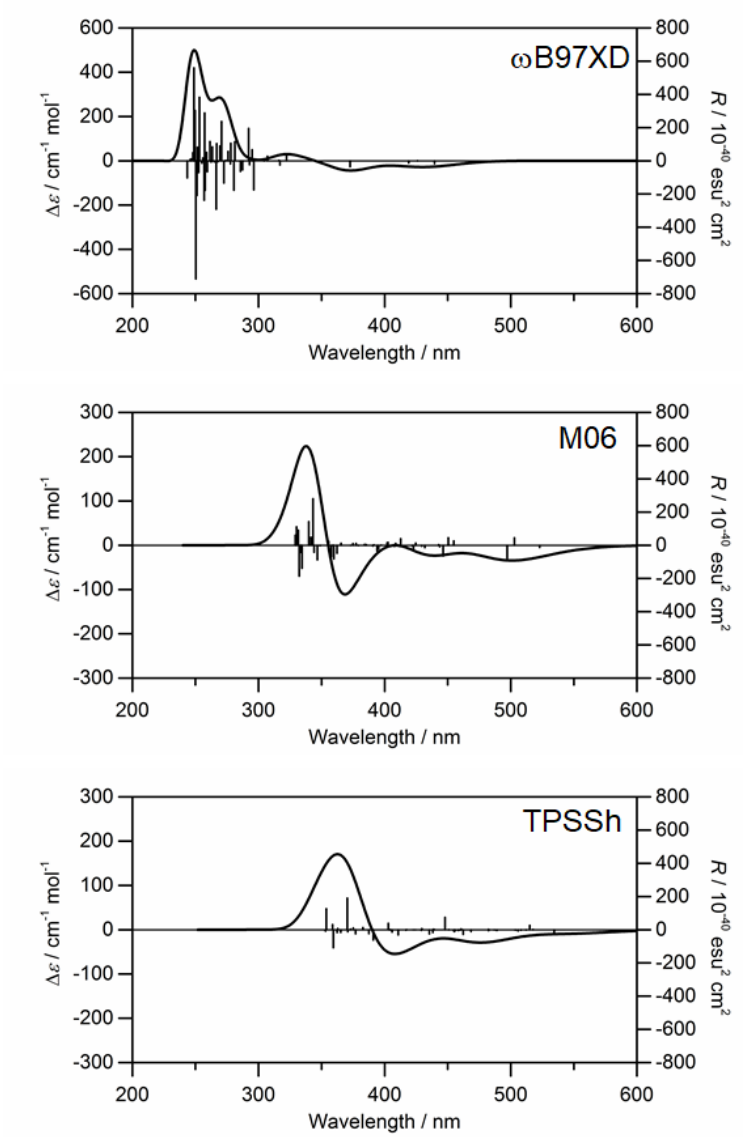

Fig. S9 Simulated CD spectra calculated with various functionals based on the optimized R-NC model.

(a)

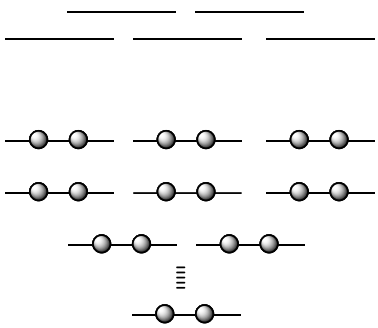

(b)

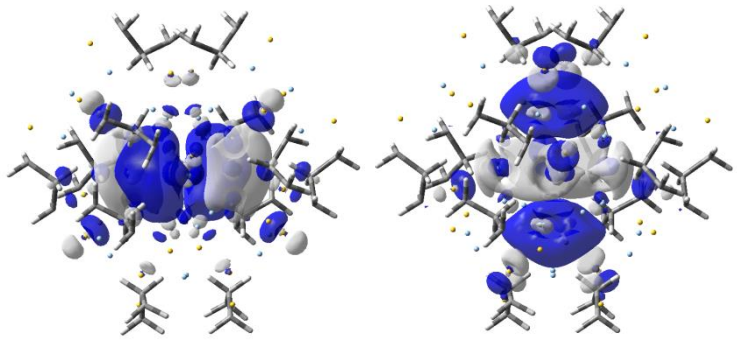

617 (LUMO+1) 618 (LUMO+1)

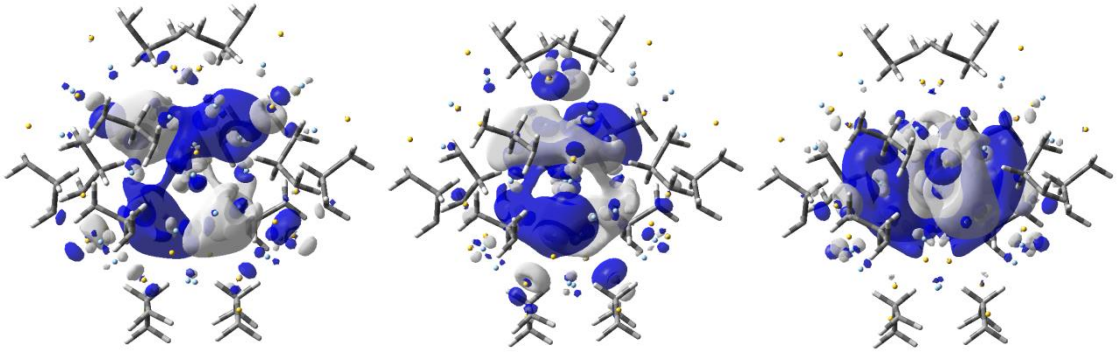

614 (LUMO) 615 (LUMO) 616 (LUMO)

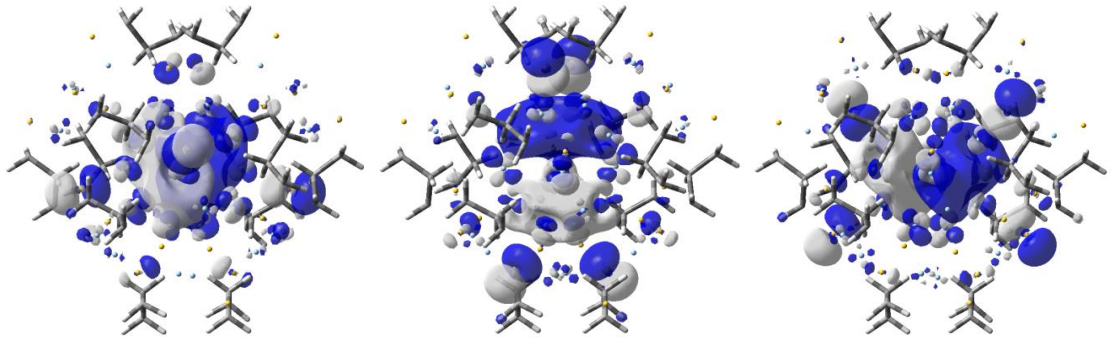

611 (HOMO) 612 (HOMO) 613 (HOMO)

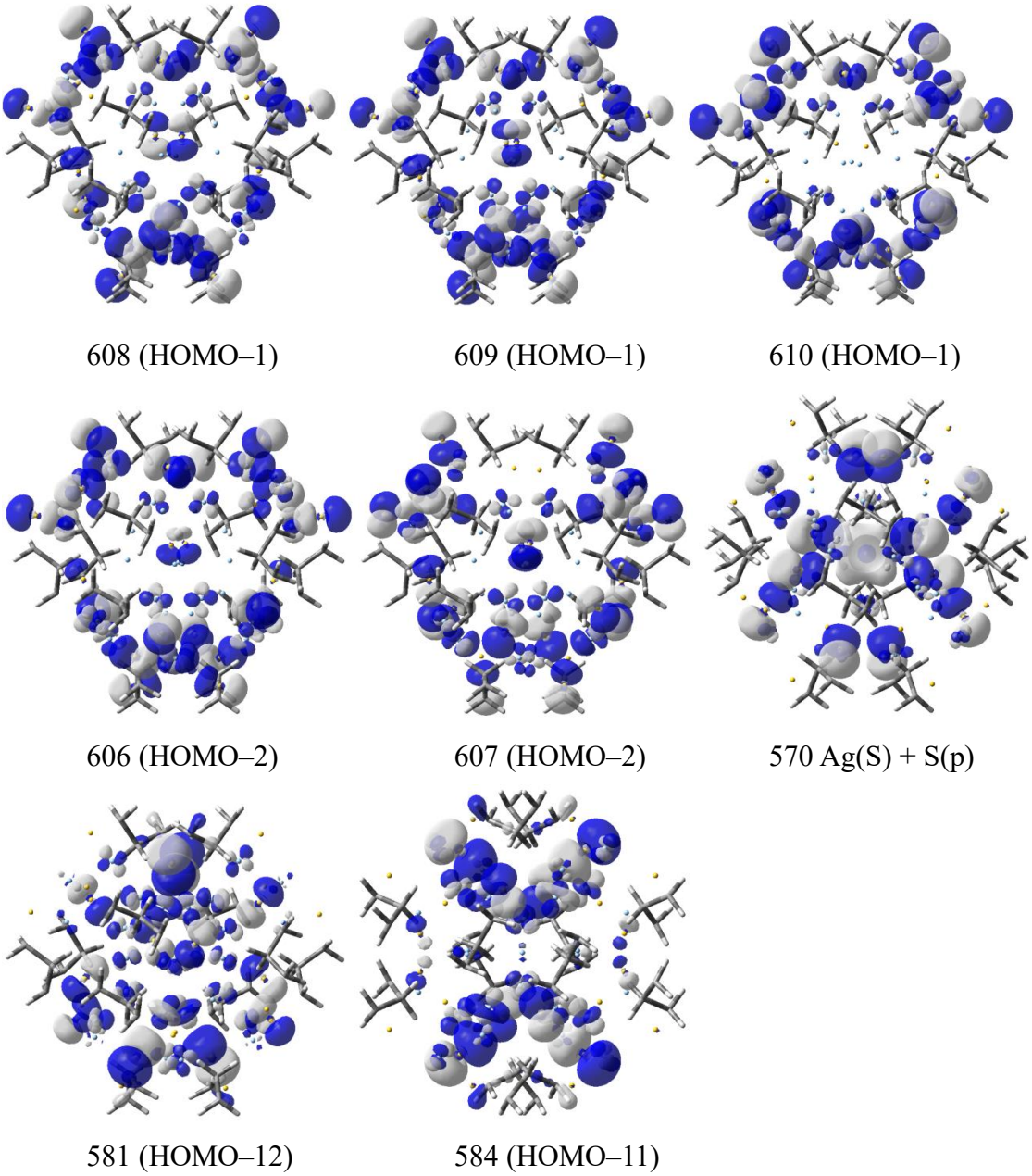

Fig. S10 (a) Orbital energy diagram and orbital character with MO numbers in the parenthesis and (b) frontier molecular orbitals of Ag_{29}(1,3–propandithiolate)$_{12}$ $^{(3-)}$.

Table S1 Excited states of right-handed structure with rotatory strength (<R>) larger than 10.0 au calculated by B3LYP/LANL2DZ(Ag)+3-21G(C, H, O, S)

State number [a]	λ_{abs} (nm)	ΔE_{abs} (eV)	<R>[b]	Transition character [c]
1–3	501	2.476	–17.5	H → L
7–9	485	2.554	23.2	H → L+1
10–12	481	2.577	–42.0	H → L+1
13–15	451	2.747	26.4	H–1 → L
31–33	430	2.885	–29.6	H–1 → L
46–48	422	2.938	–44.7	H–3 → L
54–56	411	3.015	22.3	H–3 → L
68–70	407	3.048	–12.2	H–5 → L
80–82	401	3.093	41.4	H–7 → L
83–85	394	3.147	–28.6	H–4 → L+1
95–97	391	3.168	–14.5	H–8 → L
110–112	382	3.246	–41.5	H → L+2
131–133	363	3.419	20.9	H–9 → L+1
134–136	362	3.426	–30.1	H–9 → L+1
137–139	359	3.456	–14.6	H–1 → L+2
144–146	353	3.510	–95.5	H–11 → L
148–150	351	3.528	16.1	H–11 → L
156–158	342	3.626	–80.3	H–8 → L+1
163–165	339	3.655	235.5	H–11 → L+1
171–173	336	3.688	151.6	H–4 → L+2
175–177	332	3.740	–118.9	H–12 → L+1
186–188	327	3.788	–62.9	H–7 → L+2
192–194	322	3.848	135.0	H–8 → L+2
195–197	322	3.854	18.2	H → L+2

[a] Only triply degenerate (T symmetry) states have large rotatory strength.

[b] Rotatory strength was calculated in velocity form; only one component out of three is shown.

[c] H and L represent HOMO and LUMO, respectively.

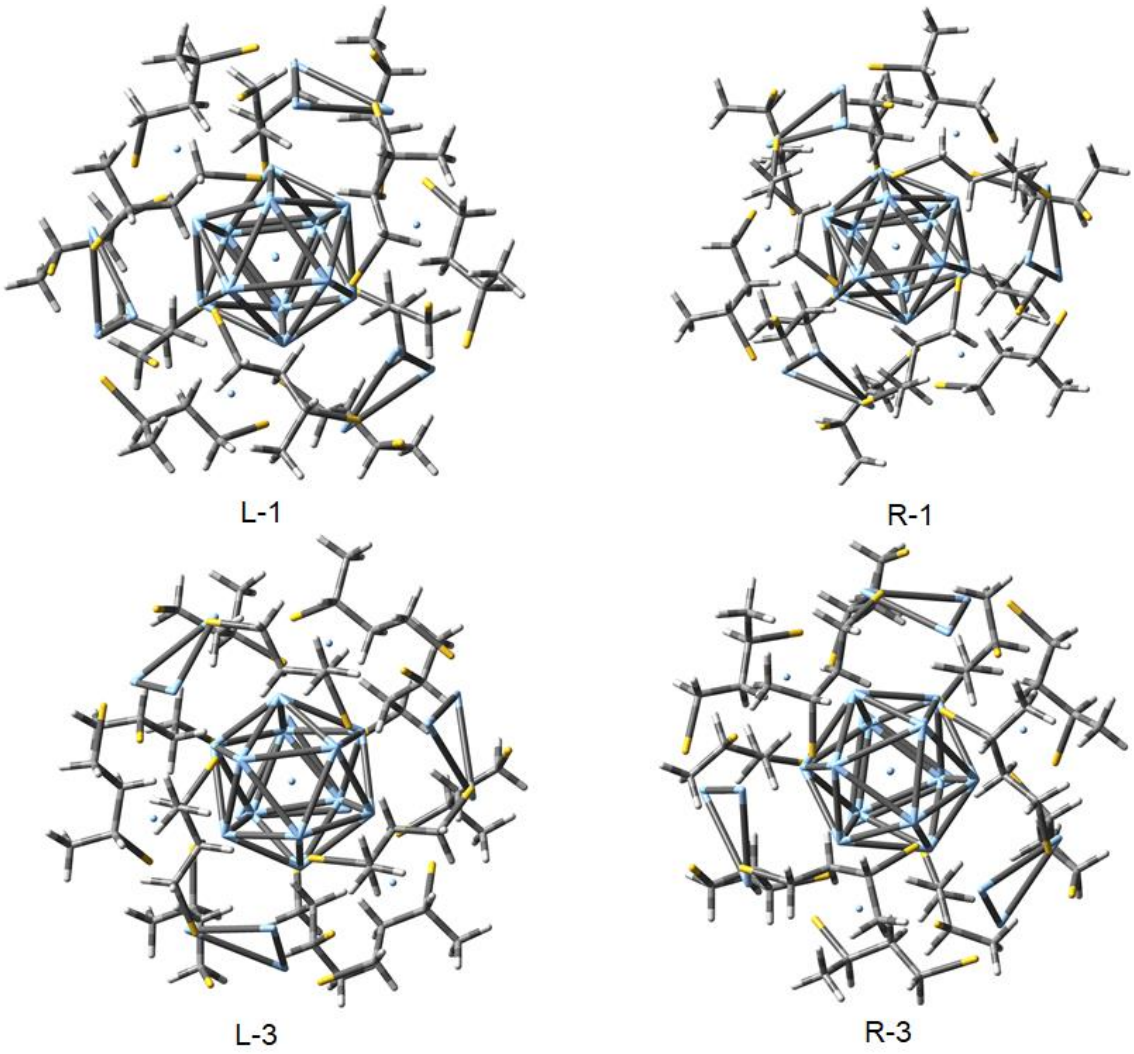

Fig. S11 Optimized structures of Ag_{29}(*R*-butane-1,3-dithiolate)$_{12}$ models.

Table S2. Energy difference among the optimized structures of Ag_{29}(*R*-butane-1,3-dithiolate)$_{12}$ models

Models	Energy(a.u.)	ΔE (kcalmol^{-1})
L-hand 1-coordination (L-1)	-15616.24770	10.50
R-hand 1-coordination (R-1)	-15616.26429	0.00
L-hand 3-coordination (L-3)	-15616.26411	0.05
R-hand 3-coordination (R-3)	-15616.22328	25.79

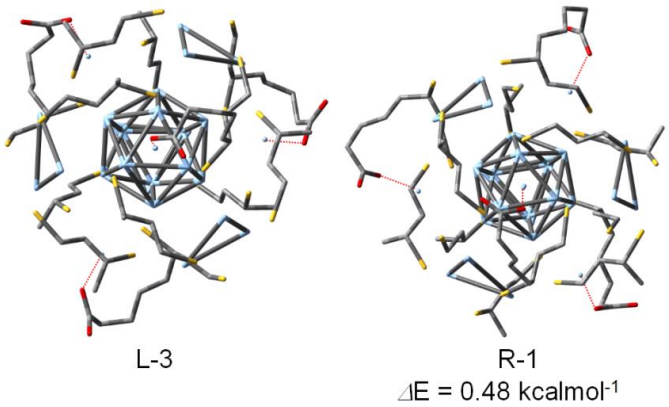

Fig. S12 Optimized structures of Ag_{29}(*R*-DHLA)$_4$(*R*-butane-1,3-dithiolate)$_8$ models with different ligand orientations (R-1 and L-3 models). Red broken lines denote coordination interactions between the silver atom and carboxylate group.

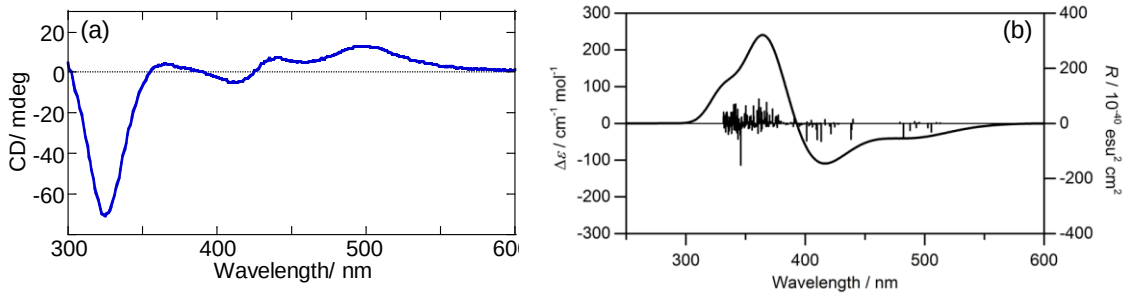

Fig. S13 Comparison of CD spectra between (a) experimental data of Ag_{29}(*R*-DHLA)$_{12}$ and (b) simulated one based on the R-1 model.

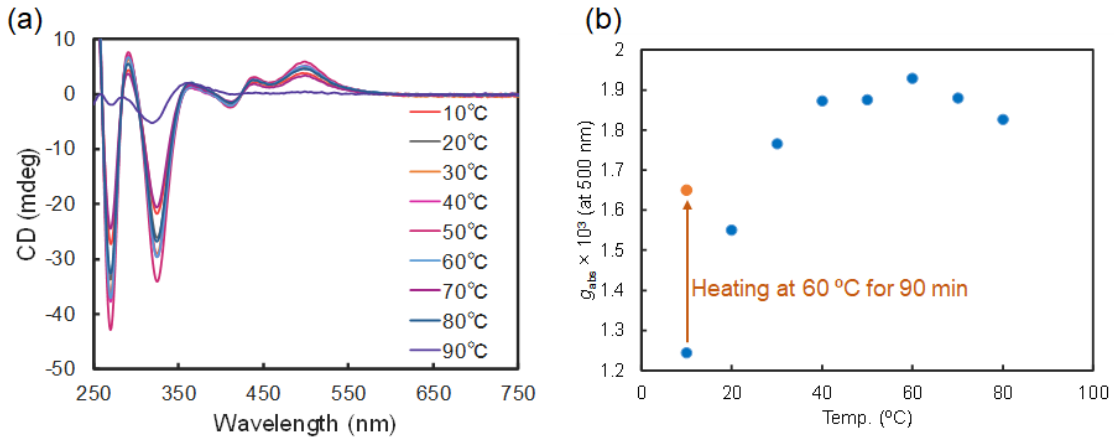

Fig. S14 (a) CD spectral change and (b) plots of g_{abs} (at 500 nm) of Ag_{29}(*R*-DHLA)$_{12}$ NCs as a function of preparation temperature.

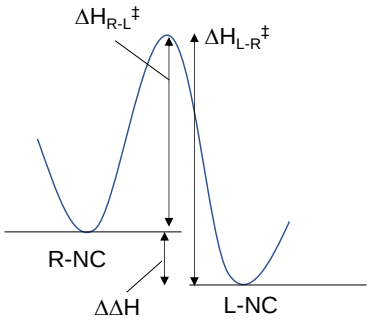

Fig. S15 Possible energy diagrams for the chirality inversion between R- and L-NCs.